FLOW ANALYSIS AND CONTROL SURFACE EVALUATION AT HIGH ANGLES OF ATTACK FOR ENHANCED MANOEUVRABILITY

D.TRISTRANT, O.RENIER, D.FARCY
ONERA-IMFL
5, Blvd Paul Painlevé
59045 LILLE CEDEX FRANCE

Abstract

Recently ONERA-IMFL has developed an experimental technique to visualize flow around an aircraft model during dynamic tests in wind tunnel. In particular flow for rotary motions of the model about velocity vector at high angles of attack is analyzed. This technique provide us with insight on behaviour of separated flow around an aircraft manoeuvring at high alpha.
Moreover, a research program has been conducted by ONERA in order to assess new means of control for combat aircraft at low speed and high angles of attack. This research program has undertaken prospective actions in which, in particular : new concepts of aerodynamic control surfaces have been designed, tested in wind-tunnel, and effectiveness of these control surfaces have been identified.
To evaluate the ability of these controls to improve flight qualities or manoeuvrability of combat aircraft at high angles of attack, a set of criteria has been designed. Some of these criteria are new, they concern specifically aerodynamics and flight mechanics at high angles of attack. More particularly, the capabilities of controls to extend the equilibrium envelope or to yield possibility to generate and to control rolls at high angle-of-attack are assessed.

Nomenclature

c	Mean aerodynamic chord
V	Aircraft velocity
Cl	Rolling moment coefficient
Cm	Pitching moment coefficient
Cn	Yawing moment coefficient
Ω	Angular velocity about velocity vector
Ω^*	Rotation rate : $\Omega^* = \Omega.c/V$
$d\Omega/dt$	Angular acceleration about velocity vector
Σ^*	Acceleration rate : $\Sigma^* = d\Omega/dt.c^2/V^2$
α	Angle of attack
β	Angle of sideslip
ρ	Air density
S	Wing reference area
I_x, I_y, I_y	Moments of inertia
A, B, C	Reduced inertia : $A=I_x/\rho\ Sc^3$
δ	Control surface deflection vector
δn	Rudder deflection

Introduction

Recent aircrafts have high swept wing, sharp leading edges and slender forebodies. At high angles of attack flow separation, burst of vortices and other complex aerodynamic phenomena occur and induce significant non-linearities in force and moment characteristics, for instance directional instabilities and lack of control effectiveness (ref 1).

A research effort has been undertaken at the Institut de Mécanique des Fluides de Lille (IMFL) to investigate and to understand the high angle of attack aerodynamics on aircraft model in dynamic motion. This will help to design the aircraft and its control devices in order to increase the stability and/or the control. Another aim of these works is to elaborate a mathematical model of the efforts taking into account the flow physics.
In this presentation the experimental tools developed by the IMFL for high angle of attack analysis will be described. Some applications will be presented : study of devices for control enhancement and experimental evaluation of their effectiveness.

A. Experimental tools for flow analysis at high angles of attack

1. Dynamic rigs

The main objective was to simulate realistic aircraft motions in order to get representative trajectories in the state- and control-space. Two main manoeuvres of combat aircraft are the rotation around the velocity axis (rolling motion) and the pitching motion. Two specific apparatus have been developed at IMFL for the analysis of aerodynamics encountered during these dynamic manoeuvres at low speed. Tests on these apparatus provide information about steady and unsteady low speed aerodynamics (ref 2-3).

1.1. "PQR" apparatus

This rig is installed in the open test section of the low speed horizontal wind tunnel (diameter = 2.4m). Its general design gives it excellent aerodynamic discretion (fig.1-2). At high alpha its main structure is installed outside the stream tube. This discretion is highly appreciable at high angles of attack at which separation of the flow and vortex breakdown occuring are known to be very sensitive to interference caused by supports and setups. This rig allows dynamic motions at high pitch rate, so dynamic effects during rapid variation of the angle of attack can be easily measured (fig.3).

Copyright © 1996 by the AIAA and ICAS. All rights reserved.

1.2. Rotary balance

This apparatus has been designed to simulate rotation on aircraft models. It is installed in the vertical wind tunnel of the IMFL (test section diameter = 4 m, maximal flow velocity = 45 m/s) (fig.4). The different degrees of freedom of this setup allow two kinds of dynamic tests (fig.5) :

-rolling motion at high angular rate and constant angles of attack and sideslip (coning motion). Therefore the damping effects can be identified.

-unsteady rotation through the use of the angle λ : angle between the flow speed direction and the axis of rotation. During these oscillatory coning motions the angles of attack and sideslip are varying so the dynamic stability parameters can be identified. The maximum angular velocity is 700°/s.

The size of the model is usually about 1 m long. Different types of model support can be used : rear sting, curved sting and top mounting.

The aerodynamic loads on the model are measured with an internal six components balance. Pressures can be also measured during the rotary tests.

2. Flow visualization at high angles of attack during dynamic motion

2.1. Objectives

The present works have been done to understand the off-surface flow around an aircraft model rotating at high angles of attack. Visualizations will complete the measures of efforts and pressures in the same domain of angle of attack and angular rate. They will be used for the development a semi-empirical model of the efforts.

At zero rotation rate this method is a complement to the surface-flow vizualisation by oil, which provides information about the location of separation and reattachment lines of the flow (fig.6).

2.2.General overview

Laser vapor screeen visualization is a technique used for many years to visualize the off-surface flow and to understand its structure. This technique is generally applied to static tests in wind tunnel. In these conditions its realisation is relatively easy. Its application to dynamic tests is more complicated. A laser light sheet, rotating with the model mounted on the IMFL rotary balance, is used to illuminate the vortical flow.

The figure 7 presents a shematic view of the experimental setup. A 4W laser generator situated outside the wind tunnel test section provides the light source which is transmitted to the static part of the rotary balance by an optical fibre and thence to the rotating arm by means of an optical rotary transmitter. A set of cylindrical lenses creates a light sheet which is parallel to the y-axis of the model. The angle between this sheet and the longitudinal axis of the model can be changed remotely to visualize the flow at different longitudinal locations, allowing the study of vortex development and breakdown over the wing.

The flow is seeded using smoke produced by oildroplets on a hot plate. The smoke is passed through a pipe to several outlets situated approximately 3 metres above the sting mount at the rear of the model. The flow is observed using a high sensibility video camera mounted above the sting mount at the rear of the model (fig. 8). The field of view of the camera is independent of the angles of attack and sideslip and of the angular rate. Signals from the camera are transmitted to a recorder by means of a gold slip ring assembly. For each video-image all the kinematic parameters of the rotary balance and therefore the angles of attack and sideslip are known.

This device has been recently installed on the "pqr" apparatus to analyze the flow during dynamic pitching motion.

2.3. Results

The model used for the tests was a delta wing combat aircraft model. This geometry was chosen for the strong vortices developing on the wing when the angle of attack increases.

2.3.1. static tests

Static tests were done at different angles of attack and for different longitudinal locations of the light sheet (fig. 9-10). These tests were made in the stall domain. The growth of the vortices over the delta wing with the angle of attack is easily visualized. When this angle reaches a certain value we can observe the vortex breakdown (the cores become much larger and dissipate in the image). These obervations will be correlated with measurements of the aerodynamic efforts or pressures to build a model of the efforts taking into account the flow physics.

The visualization of the flow around the nose shows the effects of the angle of attack on the symmetry of the vortices which develop on each side of the foredody. The aerodynamic asymmetry at high angles of attack even at zero sideslip is illustrated (fig. 11).

2.3.2 steady rotations (coning motion)

As described in upper section, the setup allows the visualization during dynamic tests. Many tests have been done to study effects of a rolling motion on the aerodynamics around the aircraft model. During these tests the angle of attack and sideslip are constant. The only changing parameter is the rate of rotation. The comparison between static tests and coning tests shows the effect of the rotation on the flow around the nose. The figure 12

presents the images obtained with the sting-mounted camera. The change of vortex position and the loss of symmetry when the model is rolling (Ω=-600°/s) are clearly illustrated.

2.3.3 unsteady rotations (oscillatory coning motion)

The strength of the vortices, their position relative to the model and location of vortex breakdown are changing as functions of angle of attack and sideslip. In dynamic tests, like oscillatory coning tests, these angles are time dependent. Owing to convective time lags there is time delays in the adjustment of the flowfield and consequent dynamic effects on measured forces. In large amplitude motion there can also be large hysteresis effects on measured coefficients. Visualizations during rotary tests will be analyzed to determine the time dependent effects.

B. Controls devices

1. Problems at high AOA

Tests were conducted on a generic combat aircraft model consisting of a delta wing with a 60° sweep angle, a single fin and a fuselage with a slender forebody nose of revolution. Control surfaces are left and right full spanned elevons and the rudder. In figure 13 static data obtained for the basic configuration give illustration of aerodynamic problems which are classically encountered in post-stall domain on slender forebody configurations. At high alpha, in addition to a loss of rudder effectiveness, a strong asymmetry of the flow appears for alpha between 40 and 60 degrees. In this alpha-range, side force and yawing moment coefficients are larger than those obtained for a full deflection of the rudder at low angles of attack. This phenomenon will promote nose slice and departure of the aircraft.

2. Experiments on high alpha aerodynamic control surfaces

The cause of the asymmetry of the side force and yawing moment has been recognized with oil surface flow visualization. At high alpha the separation lines on the forebody are asymmetric.
To fix the separation line on the forebody and therefore to control separation and location in the flow around the nose, two retractable strakes were positioned perpendicular to the forebody surface (fig.14). Each strake can be individually deployed by pivoting about an axis perpendicular to its surface and located at its apex. The basic configuration equipped with these devices will be called configuration 1. The figure 15 presents the effectiveness of these devices in yaw. When the strakes are symmetrically deployed the original asymmetry of the flow disappears.

At high alpha the rudder becomes inefficient because this control surface is totally in the wake of the fuselage and the wing (fig.16). The second concept tested consists of two keels located under the rear fuselage and therefore out of the wake of the wing (fig.17). These surfaces can deflect individually from plus or minus 20 degrees about their medium axis which is perpendicular to the fuselage surface. Because of its location a significant effectiveness of this concept was expected in a large alpha range.
Indeed the main effect of this concept was to provide control power in yaw. Its effectiveness is nearly constant in the whole alpha-range tested. However, unlike the forebody strakes, keels do not allow to get symmetry of aerodynamic loads at high alpha (fig.18). Asymmetry as encountered at zero sideslip on the basic configuration still exists. Therefore to assess efficiency of this concept on a configuration nearly symmetric at high angles of attack, the model was equipped with symmetricaly deployed forebody strakes. This configuration (rear keels and symmetric forebody strakes) is called configuration 2.

C. Evaluation of the concepts

1. Criteria

Performing rolls about velocity axis is of great interest for high angle-of-attack manoeuvrability. This motion provides possibility to quickly change the heading angle for shooting or to change flight path by tilting lift force. Moreover during this motion the angle of sideslip remains constant, contrary to rolling about longitudinal body axis because of the kinematic coupling at high angles of attack. To evaluate the efficiency of the previous tested control surfaces some criteria have been designed and applied to data basis. These criteria are defined in order to evaluate the ability of the aircraft to maintain an equilibrium flight at constant rolling rate, or to accelerate about the velocity axis at high angles of attack.

1.1 Equilibrium criterion

The equilibrium is studied essentially by considering the aircraft motion about its centre of gravity (ref.4). This analysis does not require any information about the aerodynamic forces, weight and thrust. To get equilibrium the nullity of the moments about the three body axis must be satisfied. The right hand sides of the following equations (ε_l, ε_m, ε_n) have to be equal to zero.

$$Cl(\alpha,\beta,\Omega^*,\delta) + (B-C)\,\Omega^{*2}\sin\alpha\,\sin2\beta = \varepsilon_l$$

$$Cm(\alpha,\beta,\Omega^*,\delta) + (C-A)\,\Omega^{*2}\sin2\alpha\,\cos\beta = \varepsilon_m$$

$$Cn(\alpha,\beta,\Omega^*,\delta) + (A-B)\,\Omega^{*2}\cos\alpha\,\sin2\beta = \varepsilon_n$$

At given values of alpha, beta and Ω^*, the values of (ε_l, ε_m, ε_n) depends on the control surface vector δ. The equilibrium is satisfied when the function $D1(\delta)=\sqrt{(\varepsilon_l^2+\varepsilon_m^2+\varepsilon_n^2)}$ is equal to zero. The equilibrium criterion, called E, is chosen as the minimum value of D1

on the set of δ values : $E=\min_\delta D1(\delta)$.
This criterion qualifies the capability of the control surface deflection vector to equilibrate aircraft. As E is equal to zero, equilibrium is achieved, otherwise the value of E represents the deviation from equilibrium with dimension of aerodynamic coefficient. E criterion gives an evaluation of the control surface efficiency.

Values of E criterion have been computed for the basic configuration and for configurations 1 and 2. For the basic configuration the control surface deflection vector is componed of the three conventional control surfaces : elevons and rudder. For the configuration 1 the settings of the two independent forebody strakes are added to the control vector. For the configuration 2 the control surface vector comprises the two keel settings in addition to elevons and rudder settings (the strakes are fixed and fully deployed).
Values of E criterion are represented in the (α,β) plane by a grey level : the higher the value, the darker the grey level. The white area corresponds to values close to zero. On this domain the equilibrium condition is satisfied or can be considered so regarding accuracies involved.

Firstly equilibria at zero rotation rate are studied. Comparison between the three configurations (fig. 19) shows the extension of the equilibrium area in the high alpha range with the two tested concepts. On the basic configuration the maximum value of angle of attack where equilibrium is achieved is about 45 degrees. This value is enlarged up to 60 degrees with the added control surfaces. The equilibrium area is widely extended.

The same comparison is made when the aircraft is in rolling motion. The numeric value of $\Omega^*=0.07$ which is chosen for application corresponds to an angular velocity of 50°/s at a speed of 100 m/s. Figure 20 presents the results of the E criterion for each configuration. It appears that the equilibrium domain is much larger for the aircraft fitted with the two concepts than for the initial configuration.

1.2. Acceleration rate criterion

Capability of quickly accelerating or decelerating rolls around velocity axis in flight is also of great interest. The same assumptions are made as for E equilibrium definition: only moments about body axes are considered. The pitching equation is not taken into account, because capability of concepts 1 and 2 to accelerate or deccelerate rolls is estimated only on the roll and yaw axes. Moreover contribution of the acceleration rate is fairly small on the pitching moment equation in comparison to yawing and rolling moments since it is proportional to sine beta.
So, to create an acceleration rate about the velocity vector, called Σ^*, the two following moment equations must be satisfied :

$$\frac{1}{2A}Cl(\alpha,\beta,\Omega^*,\delta)+\frac{B-C}{2A}\Omega^{*2}\sin\alpha\sin2\beta - \Sigma^*\cos\alpha\cos\beta= \varepsilon_l$$

$$\frac{1}{2A}Cn(\alpha,\beta,\Omega^*,\delta)+\frac{A-B}{2A}\Omega^{*2}\cos\alpha\sin2\beta - \Sigma^*\sin\alpha\cos\beta= \varepsilon_n$$

As previously for equilibrium moment equations, at given values of alpha, beta, Ω^* and Σ^*, a metric $D2(\delta)=\sqrt{(\varepsilon_l^2+\varepsilon_n^2)}$ can be defined from the two acceleration rate equations. An acceleration rate criterion, called AR, is defined as following : $AR=\min_\delta D2(\delta)$
Figure 21 presents the values of AR criterion in the (α,β) plane for the three configurations. The calculations have been made for an adimensional acceleration rate Σ^* equal to 0.007 at zero rotation rate. This corresponds to an acceleration rate close to $60°/s^2$ at a velocity of 100 m/s which are realistic values for a combat aircraft. The grey scale representation is the same as previously.

For the basic configuration, AR criterion is satisfied up to 40 degrees in angle of attack at zero sideslip. Because of directional instability at high alpha, sideslip to the left tends to yaw aircraft to the right. Negative sideslip tends therefore to promote positive acceleration rate. That explains the asymmetry of the domain where AR criterion is satisfied.
For configuration 1 this area is largely extended. Asymmetry with sideslip can be explained as previously. This area is not significantly extended for the configuration 2 because of the limited control power in yaw of this concept.

2. Free model flight tests

Free model flight tests have been performed in a specific laboratory of the IMFL (fig.22). The objectives were to validate the efficiency of the yaw control devices. The model is launched at high angle of attack, which is the domain where the strakes have their maximum effect and other classical yaw control devices are inefficient. Tests have been done for different positions of the strakes. The yaw rate measured during the flight confirms the measurements in wind tunnel : with the strakes deployed on each side of the forebody the flight remains symmetric, without these devices the yaw rate increases during the flight due to the aerodynamic asymmetry on the forebody (fig.23). The yaw rate of the model can be controled by deploying only one strake : for instance the model yaws to the right when the left strake is deployed.

Conclusion and perspectives

Test on two specific dynamic apparatus in wind tunnel have been carried out on a generic delta wing aircraft model to provide information about steady and unsteady aerodynamics during rolling and pitching motion. Flow visualization is used to complete the measurements of

aerodynamic loads and to understand the flow structure at high angles of attack. A device has been installed on the rotary balance for visualization during rotary tests. Analysis of separated flow and vortices around an aircraft model rotating at high angles of attack is therefore achieved. These results are planned to be used for the near future for building a mathematical model of the aerodynamic loads taking into account the flow physics at high angles of attack.

The yaw control at high angles of attack is often very low because of the strong flow asymmetries and the lack of control effectiveness of the rudder. Two different concepts of aerodynamic surfaces for control in yaw have been tested and compared. The first one consists in two retractable strakes, located on the forebody for fixing the flow separation lines and therefore modifying the original asymmetry of the flow at high angles of attack. The second concept is under the rear fuselage, and is therefore efficient at high alpha for yaw control, when the rudder is completely in the wake of the wing.

To evaluate power and efficiency of these concepts flight mechanics criteria are proposed. These criteria provide information on capability of concepts :

- to balance aircraft rolls around the velocity vector ;
- to increase or decrease the aircraft rotation rate about the velocity vector.

Comparisons between the two concepts results show that controling forebody vortices seems to be a more efficient way to control yaw at high angles of attack.

References

1. G.N.Malcolm "Forebody Vortex Control" in "Aircraft dynamics at high AOA : experiments and modelling" AGARD Report n°776 Paper 6
2. O.Renier "Characterisation of unsteady aerodynamic phenomena at high AOA" in "Manoeuvring dynamics" AGARD CP497, May 1991, Paper 11
3. O.Renier "Outils pour la caractérisation aérodynamique et l'évaluation des performances à haute incidence" in "Technologies for highly manoeuvrable aircraft" AGARD CP548 October 1993
4. D.Tristrant "Evaluation of new or recent control surfaces for flight at high angles of attack" Workshop on "Full envelope agility" 4-PWR SMTG 29-30 March 1995 Eglin, Florida

Figures

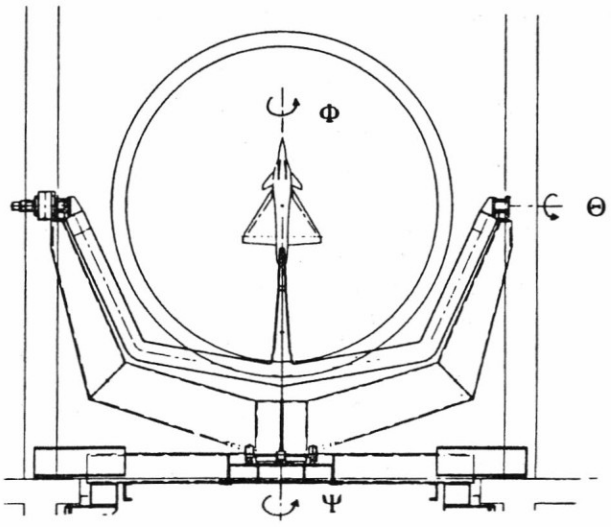

Fig.1 : Dynamic apparatus "PQR". Shematic view

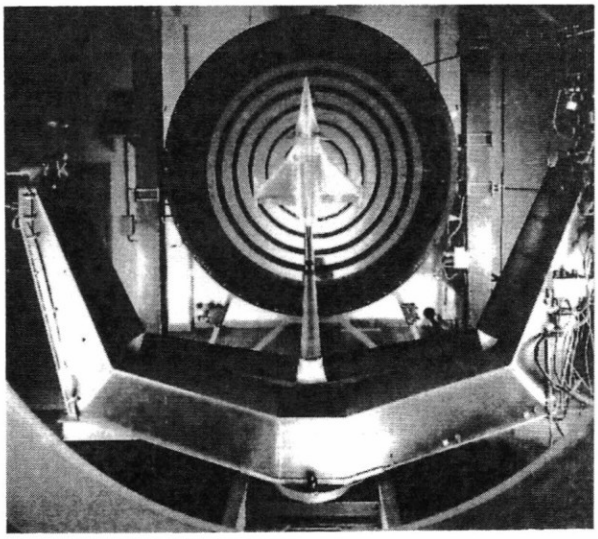

Fig.2 : Aircraft model on the dynamic apparatus "PQR"

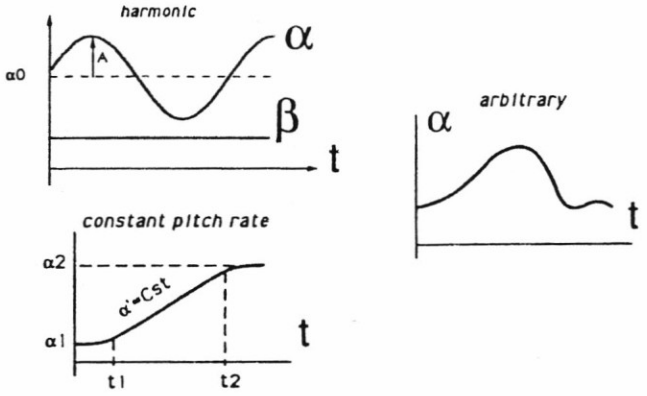

Fig.3 : Dynamic tests on the dynamic apparatus "PQR". $\alpha(t)$, $\beta(t)$

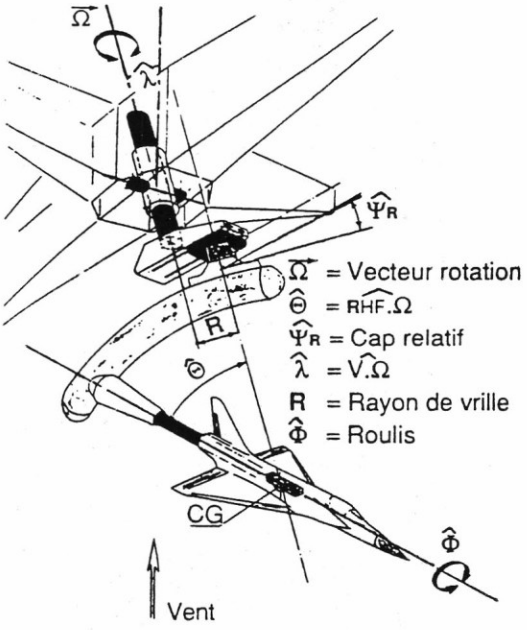

Fig.4 : Rotary balance. Shematic view

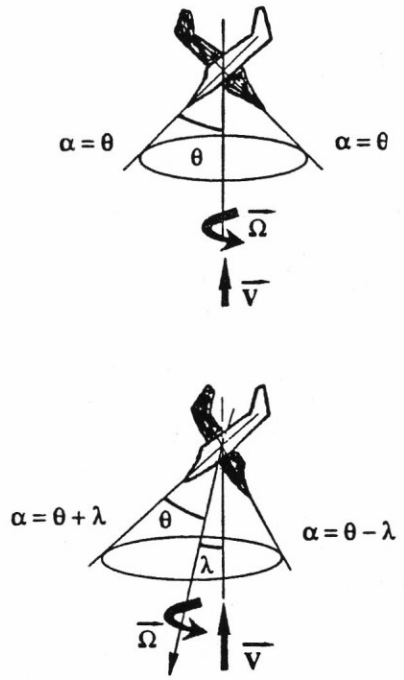

Fig.5 : Coning and oscillatory coning motions on rotary balance

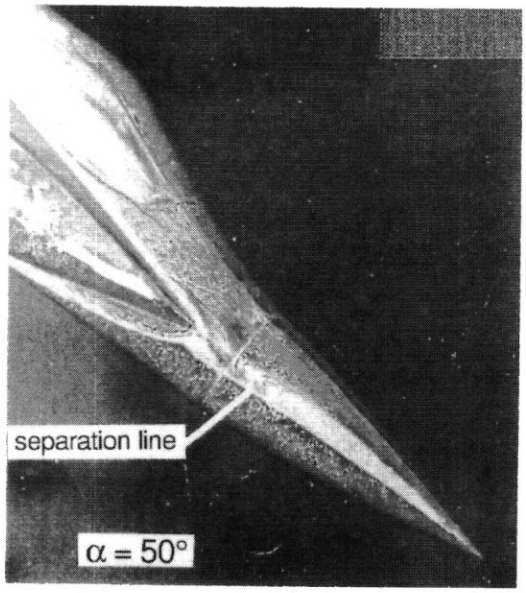

Fig.6a : Effect of strakes on forebody flow pattern
Clean forebody

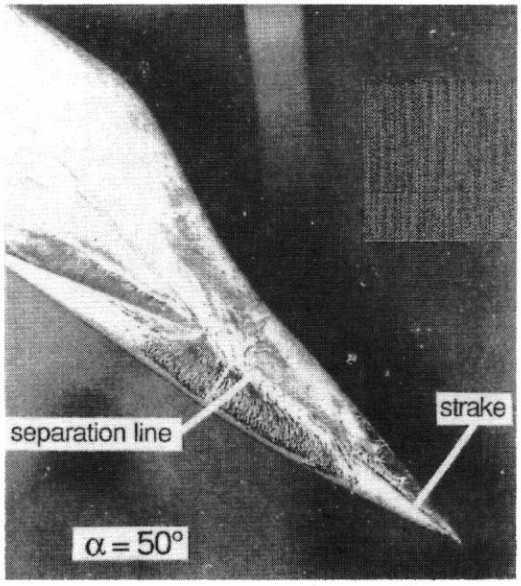

Fig.6b : Effect of strakes on forebody flow pattern
Forebody equipped with a single right hand strake

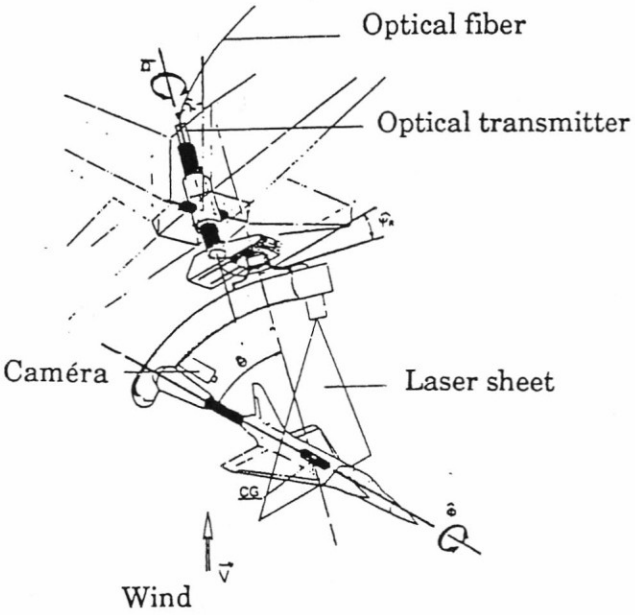

Fig.7 : shematic view of the setup for visualization on rotary balance

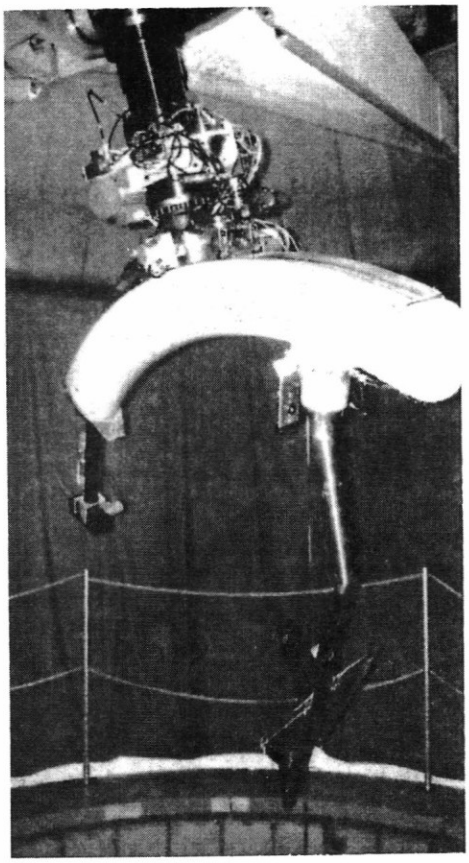

Fig.8 : Visualization during rotary tests : experimental setup

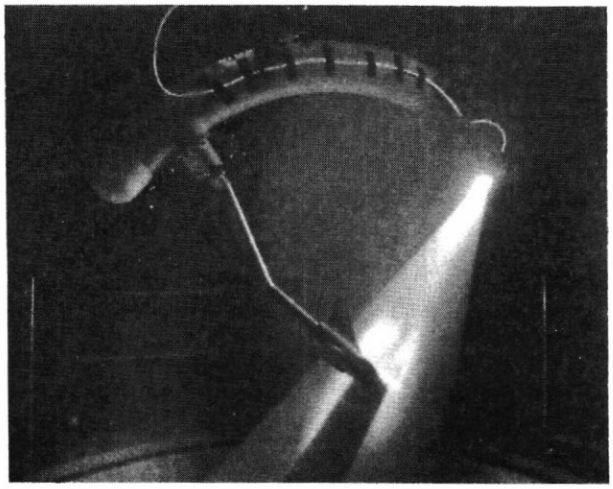

Fig.9 : Visualization during rotary tests

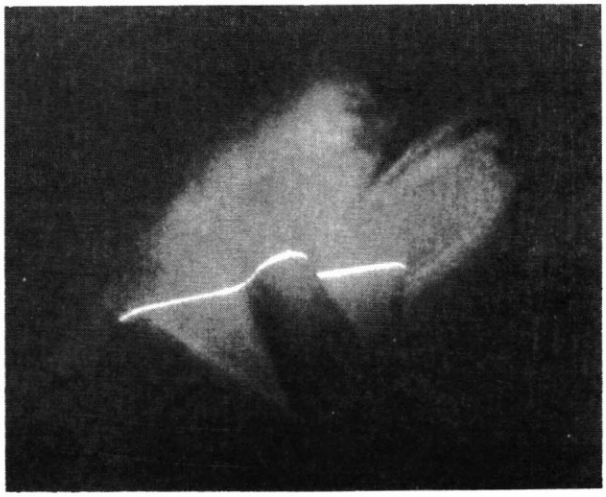

Fig.10 : Visualization during rotary tests : vortices over delta wing

Fig.11 : asymmetric flow on forebody at high alpha

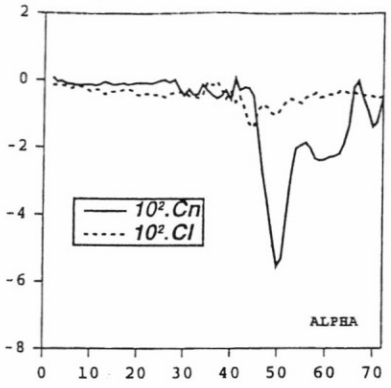

Fig.13 : Asymmetry at zero sideslip. Basic configuration

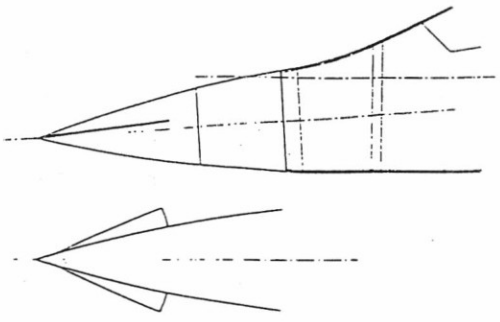

Fig.14 : Forebody strakes on basic configuration

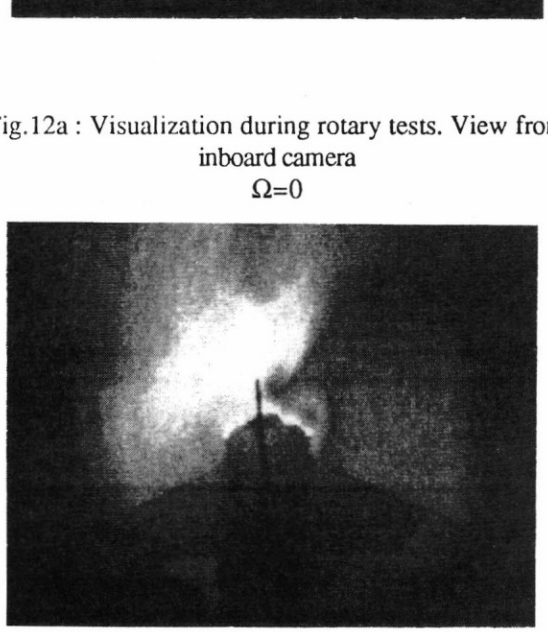

Fig.12a : Visualization during rotary tests. View from inboard camera
Ω=0

Fig.12b : Visualization during rotary tests. View from inboard camera
Ω=-600°/s

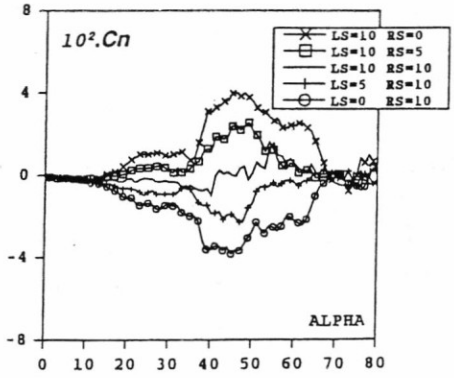

Fig.15 : Forebody strakes effectiveness in yaw

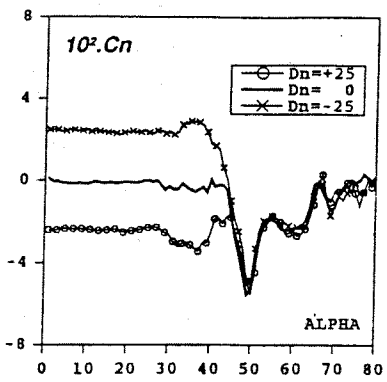

Fig.16 : Rudder effectiveness in yaw

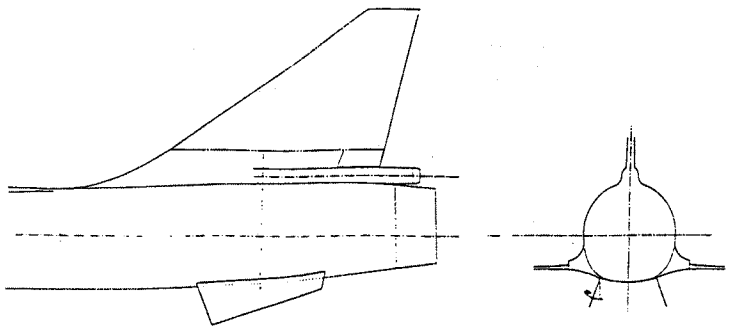

Fig.17 : Rear keels on basic configuration

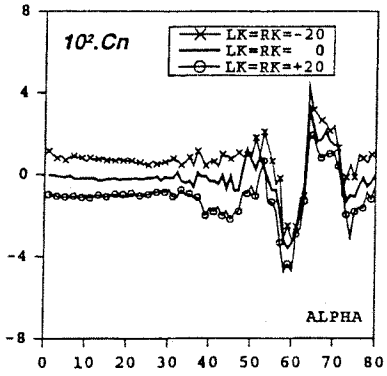

Fig.18b : Rear keels effectiveness in yaw without strakes

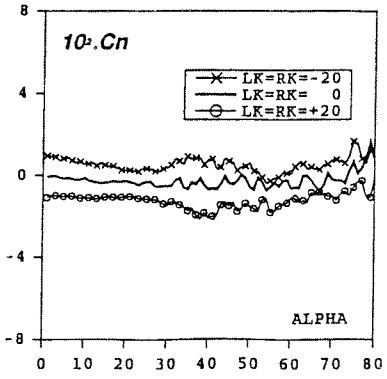

Fig.18b : Rear keels effectiveness in yaw with deployed strakes

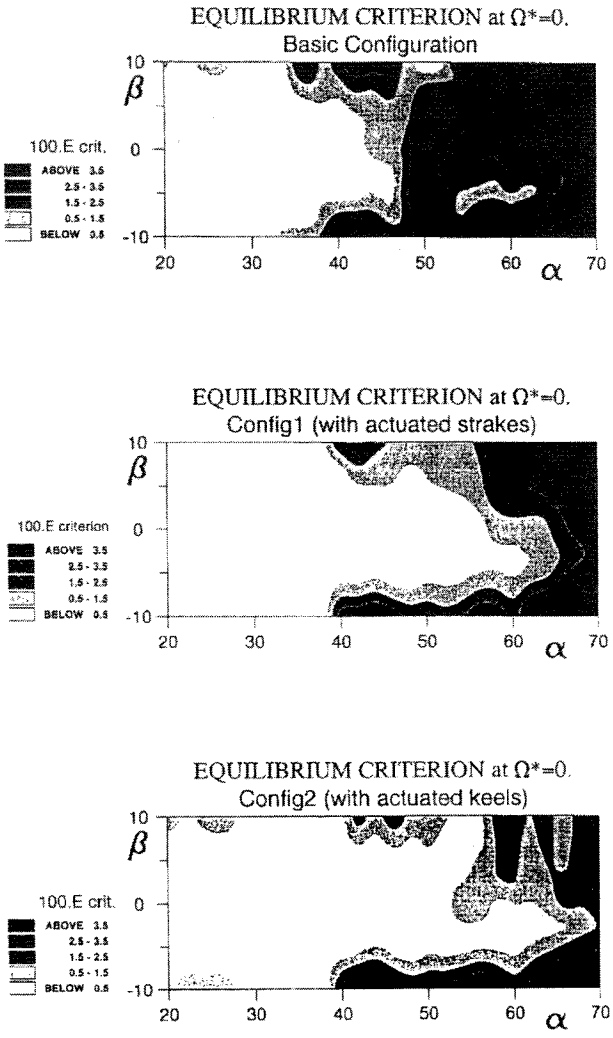

Fig.19 : Equilibrium criterion at zero rotation rate. Comparison of the configurations

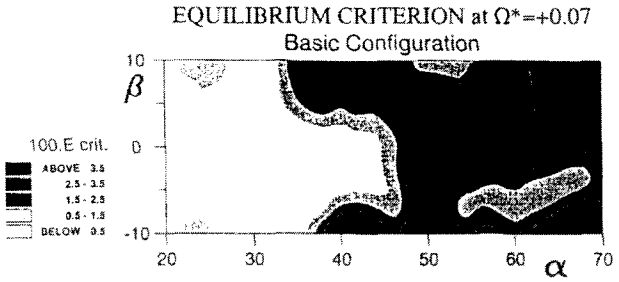

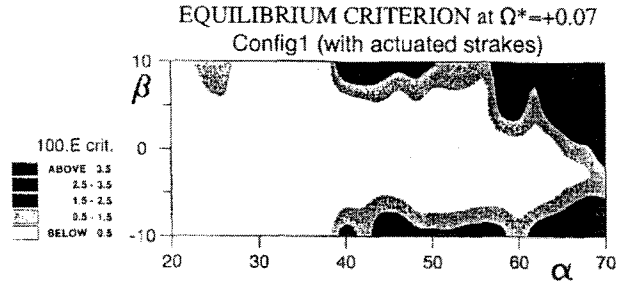

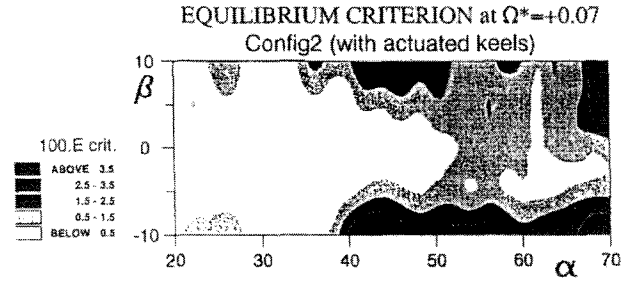

Fig.20 : Equilibrium criterion at Ω*=0.07. Comparison of the configurations

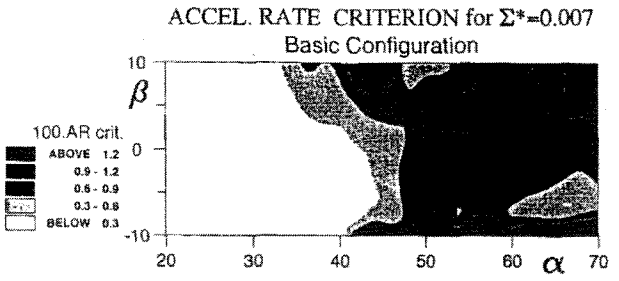

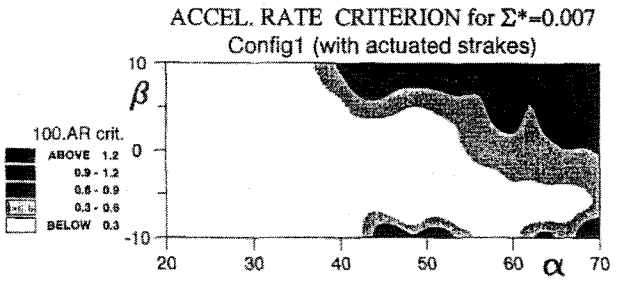

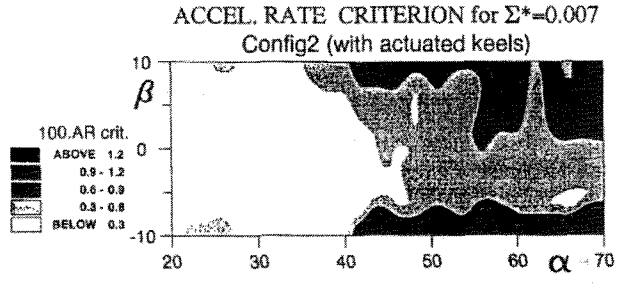

Fig.21 : Acceleration rate criterion at Ω*=0, Σ*=0.007. Comparison of the configurations

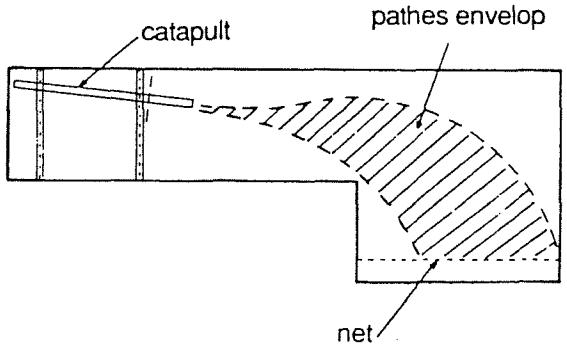

Fig. 22 : Free model flight laboratory

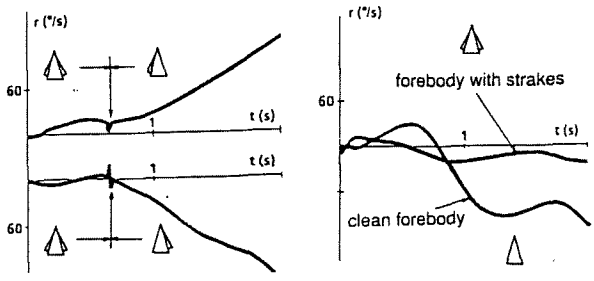

Fig. 23 : Effects of strakes on yaw control r(t)